Supporting Information

Riemer et al. 10.1073/pnas.0900742106

SI Text

Target Sequences for siRNA Directed Against ERFAD mRNA (5′–3′).

#1: TCG AGC TAG CTA CGA ATC CAA
#2: CAG GAC GAC AAT GAC AAC TTT
#3: CCC GCT GAT TCG AGC TAG CTA
#4: CAA GGC TAA CGC CGA GTT CAA
Control: AAT TCT CCG AAC GTG TCA CGT

AMS Modification. The in vivo redox state of the PDI-family members TMX3 and ERp57 was determined using 4-acetamido-4-maleimidylstilbene-2,2-disulfonic acid (AMS) to alkylate free thiols (1, 2). The redox state in vivo was trapped by alkylation of free thiols with 20 mM *N*-ethylmaleimide (NEM), and the cells were lysed in 80 mM Tris·HCl containing 100 mM NaCl, 2 mM EDTA, and 2% (wt/vol) SDS. The lysate was denatured by boiling for 2 min. Tris[2-carboxyethyl]phosphine (TCEP) was added (10 mM) to break existing disulfide bonds, which were then alkylated by the addition of 25 mM AMS (Molecular Probes) for 1 h at room temperature. By this assay, proteins containing disulfide bonds will be modified with AMS which results in a slower migration on SDS/PAGE.

mPEG-mal Modification of PDI and ERdj5. The in vivo redox state of PDI was determined as described in ref. 2. Cells grown in six-well plates were overnight pulse labeled, subjected to in situ NEM-alkylation and lysed in buffer containing SDS and denatured for 60 min at 97 °C. Subsequently, NEM was added to a final concentration of 20 mM, and the mixture was incubated at room temperature for 1 h. Then, an immunoprecipitation with anti-PDI was performed and proteins were released from the beads by boiling in 50 μL 80 mM Tris·HCl, pH 7.0, 2% SDS. Forty microliters of the resulting supernatant was transferred to a tube containing 2 μL of 200 mM TCEP ($\approx$10 mM final concentration) and incubated for 15 min at room temperature to reduce active-site disulfides. Thus, reduced cysteine residues were then alkylated for 1 h at room temperature in 15 mM mPEG-mal. Excess mPEG-mal was removed by methanol/chloroform protein precipitation. Using this procedure, in vivo-oxidized cysteine residues will be modified with mPEG-mal, which in turn will result in decreased gel mobility.

The in vivo redox state of ERdj5 was determined as follows: HEK293 cells were pulsed with [^{35}S]methionine (Perkin–Elmer) for 16 h, washed with cold PBS, covered with 10% TCA, and incubated on ice for 15 min. The precipitated cell material was then scraped from the culture dish with a rubber policeman, pelleted at 20,000 $\times$ *g* at 4 °C for 15 min and the pellet covered with a solution containing 58 mM Tris·HCl, pH 7, 27% dimethyl sulfoxide, 7.3% glycerol, 1.5% SDS, 15 mM methoxy polyethylene glycol-maleimide 5000 (mPEG-mal, Laysan Bio) 0.2 mM phenylmethylsulfonylfluoride, and 0.1% bromcresol purple. After neutralization of the supernatant by dropwise addition of 1 M Tris/Cl, pH 8, until the solution turned purple, the pellet was solubilized using a microsonicator equipped with a 0.5 mm sonotrode (Hielscher Ultrasound Technology) followed by incubation at room temperature for 1 h. Ten sample volumes of cold 30 mM Tris·HCl, pH 8.1, 100 mM NaCl, 5 mM EDTA, and 2% Triton X-100 were then added, and the lysate processed for anti-ERdj5 immunoprecipitation.

When performed in this manner, without the in situ NEM alkylation step and the TCEP incubation used in the case of PDI, but with direct TCA treatment, it is the in vivo-reduced cysteine residues that will become modified with mPEG-mal.

Splicing of XBP1 mRNA. The splicing of XBP1 mRNA was analyzed as described in ref. 3. Appearance of the spliced product indicates induction of the Ire1 pathway of the unfolded protein response (UPR).

Mass Spectrometry. SEL1L was identified from SDS/PAGE gel bands as follows: First, protein bands were excised and in gel digestion was performed as described in ref. 4. Then the peptide mixtures were analyzed on a linear ion trap mass spectrometer (LTQ, Thermo) interfaced with an electrospray ion source. Chromatographic separation of peptides was achieved on an Agilent Series 1100 LC system (Agilent Technologies), equipped with an 11-cm fused silica emitter, 100-μm inner diameter (BGB Analytik), packed in-house with a Magic C18 AQ 5 μm resin (Michrom BioResources). Peptides were loaded from a cooled (4 °C) Agilent auto sampler and separated with a linear gradient of acetonitrile/water, containing 0.15% formic acid, with a flow rate of 0.95 μL/min. Peptide mixtures were separated with a gradient from 5 to 30% acetonitrile in 90 min. For each peptide sample a standard data-dependent acquisition method on the three most intense ions per MS scan was used and a threshold of 10,000 ion counts was used for triggering an MS/MS attempt.

Data Analysis. The MS/MS data were searched against the human National Cancer Institute nonredundant database from 18.12.2004 using the Comet algorithm (5). For the in silico digest of the protein database trypsin was defined as protease, cleaving after K and R (if followed by P the cleavage was not allowed). Two missed cleavages and one nontryptic terminus were allowed for the peptides, which had a maximum mass of 6,000 Da. The precursor ion tolerance was set to 3 Da and fragment ion tolerance was set to 0.5 Da. Finally, search results obtained by the Comet algorithm were analyzed by the transproteomic pipeline (6, 7).

Plasmids and Primers. For plasmids and primers see Table S1.

The Redox State of ERdj5. The ERdj5 in vivo redox state has not previously been investigated. Interestingly, the vast majority of ERdj5 is oxidized at steady state (Fig. S4*H*). We also show that the ERdj5 redox state is seemingly not affected by the knockdown of ERFAD, although this were perhaps to be expected based on the detected interaction between the two proteins. However, because ERdj5 contains four thioredoxin-like domains with active-site CXXC motifs, the protein can—in addition to the completely oxidized and reduced states—exist in a variety of semioxidized forms where the redox state of the various domains differ. As observed for PDI, where the two semioxidized forms migrate differently despite both having one active site oxidized and the other reduced (2), these many redox forms likely run differently by SDS/PAGE. Although the reduced and oxidized forms clearly appear in the control lanes, we detected only very weakly one semioxidized form (Fig. S4*H*, lanes 3 and 4; arrowheads). Still, there might be even lower levels of other semioxidized forms present in the cell that we do not detect. This assay therefore does not provide sufficient information to state anything definite about a potential change in the redox state of ERdj5 upon down-regulation of ERFAD. At present we can only conclude that no change occurs to significantly lower the level of the fully oxidized state. This does not rule out that ERFAD could control the redox state of one particular active site (and not the remaining three). The inves-

tigation of this possibility would require mutants with active-site cysteines changed to Ser or Ala in three of four thioredoxin-like domains. These four mutants should then be tested as potential substrates for ERFAD.

1. Haugstetter J, Blicher T, Ellgaard L (2005) Identification and characterization of a novel thioredoxin-related transmembrane protein of the endoplasmic reticulum. *J Biol Chem* 280:8371–8380.
2. Appenzeller-Herzog C, Ellgaard L (2008) In vivo reduction-oxidation state of protein disulfide isomerase: The two active sites independently occur in the reduced and oxidized forms. *Antioxid Redox Signal* 10:55–64.
3. Yoshida H, Matsui T, Yamamoto A, Okada T, Mori K (2001) XBP1 mRNA is induced by ATF6 and spliced by IRE1 in response to ER stress to produce a highly active transcription factor. *Cell* 107:881–891.
4. Shevchenko A, Tomas H, Havlis J, Olsen JV, Mann M (2006) In-gel digestion for mass spectrometric characterization of proteins and proteomes. *Nat Protoc* 1:2856–2860.
5. Keller A, Eng J, Zhang N, Li XJ, Aebersold R (2005) A uniform proteomics MS/MS analysis platform utilizing open XML file formats. *Mol Syst Biol* 1:2005 0017.
6. Keller A, Nesvizhskii AI, Kolker E, Aebersold R (2002) Empirical statistical model to estimate the accuracy of peptide identifications made by MS/MS and database search. *Anal Chem* 74:5383–5392.
7. Nesvizhskii AI, Keller A, Kolker E, Aebersold R (2003) A statistical model for identifying proteins by tandem mass spectrometry. *Anal Chem* 75:4646–4658.
8. Mezghrani A, et al. (2001) Manipulation of oxidative protein folding and PDI redox state in mammalian cells. *EMBO J* 20:6288–6296.
9. Misaghi S, Pacold ME, Blom D, Ploegh HL, Korbel GA (2004) Using a small molecule inhibitor of peptide: N-glycanase to probe its role in glycoprotein turnover. *Chem Biol* 11:1677–1687.
10. Baker BM, Tortorella D (2007) Dislocation of an endoplasmic reticulum membrane glycoprotein involves the formation of partially dislocated ubiquitinated polypeptides. *J Biol Chem* 282:26845–26856.

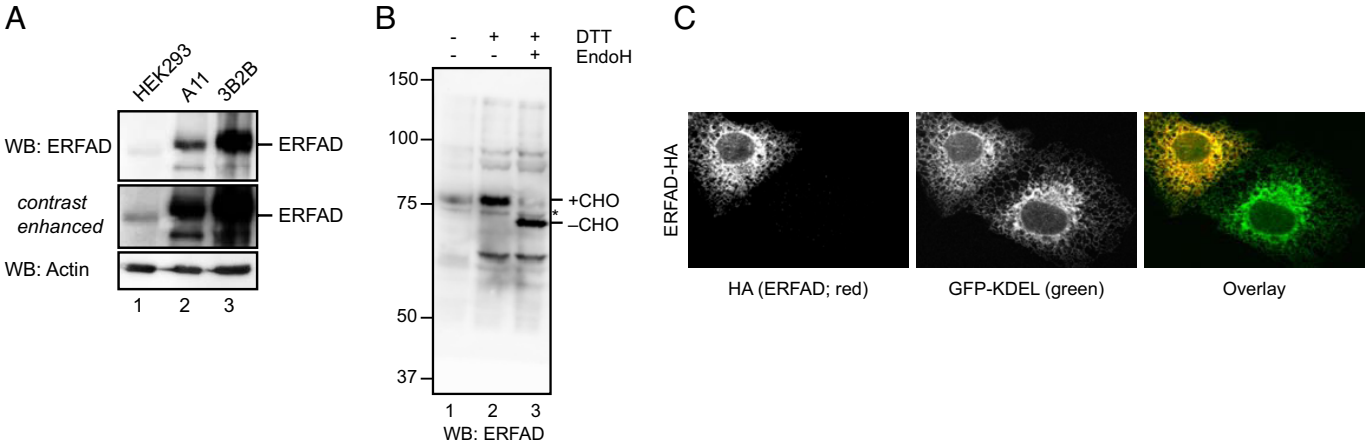

Fig. S1. Additional basic characterization of ERFAD. (*A*) Expression levels of ERFAD in HEK293, A11, and 3B2B cells. Cell lysates were adjusted to the same protein concentration and blotted with anti-ERFAD and anti-actin. (*B*) The complete Western blot analysis of Fig. 1*E* is shown. *, background band, corresponds to the background band labeled on ERFAD blots throughout the manuscript. (*C*) Immunofluorescence microscopy of ERFAD-HA in VERO cells. Cells were cotransfected with pcDNA3/ERFAD-HA and a plasmid encoding the ER marker GFP-KDEL (*Center*, green), fixed, and stained with anti-HA (*Left*, red). A merged image is shown in the *Right*.

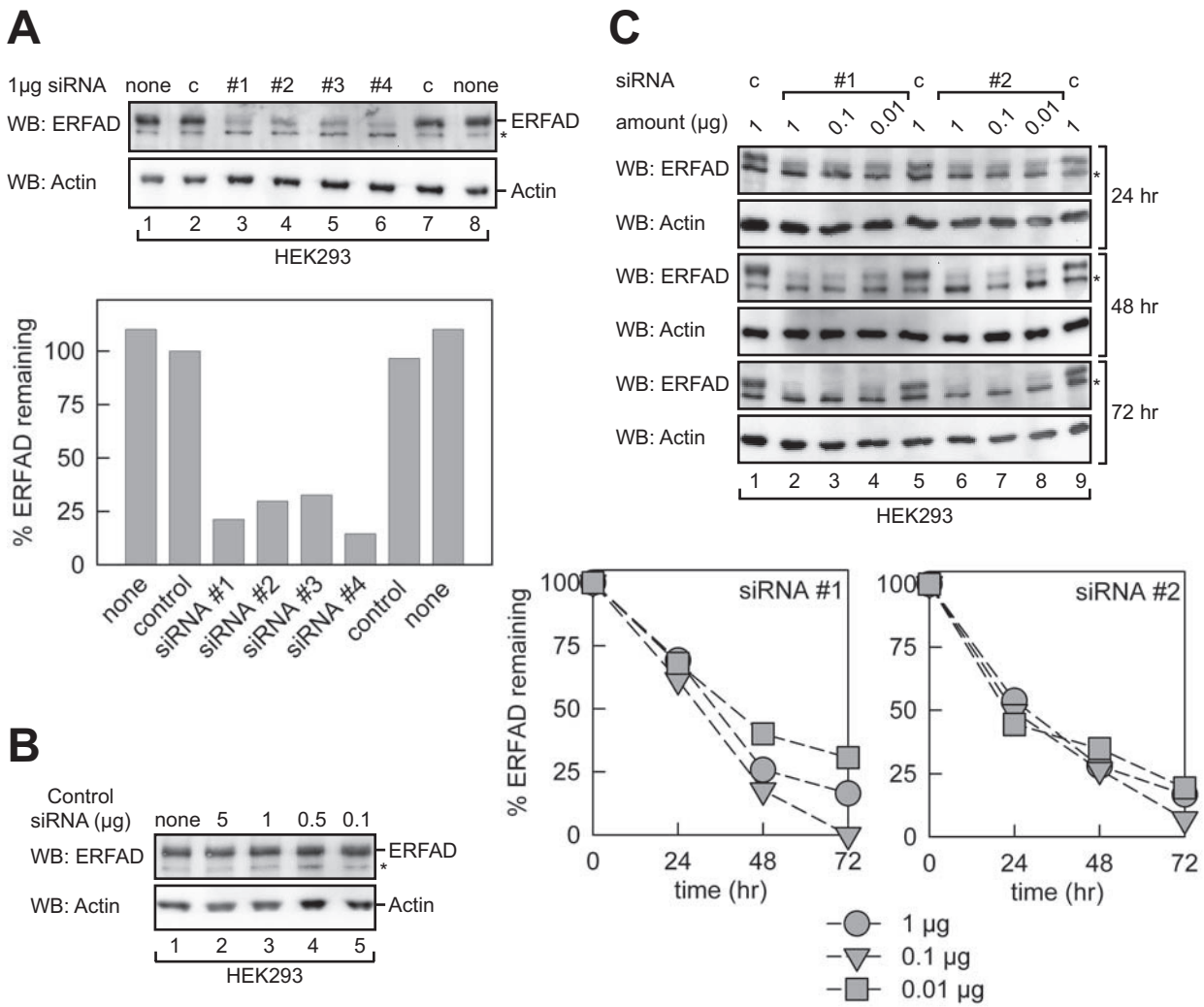

Fig. S2. Establishment of ERFAD knockdown. (*A*) Knockdown of ERFAD with four different siRNAs. HEK293 cells were transfected using the calcium phosphate transfection method with four different siRNAs directed against ERFAD (#1-#4; 1 μg per 35-mm dish) as well as a nonsilencing control siRNA (c; 1 μg per 35-mm dish). Cells were lysed 48 h after transfection and the lysates analyzed by Western blotting with antibodies against ERFAD and actin. A background band in the Western blot against ERFAD is labeled with an ∗. The bar diagram shows the quantification of the experiment. (*B*) Transfection of nonsilencing siRNA (control) into HEK293 cells. As in *A*, except that HEK293 cells were transfected with different amounts of nonsilencing control siRNA. (*C*) Establishment of optimal siRNA concentration and transfection time for ERFAD knockdown. As in *A*, except that HEK293 cells were only transfected with siRNAs#1 and #2, but in different amounts as well as a nonsilencing control siRNA (c). In addition, cells were lysed 24, 48, and 72 h after transfection. The graphs show the quantification of the experiments. Subsequently, we performed all experiments 72 h after transfection with 0.1 μg siRNA.

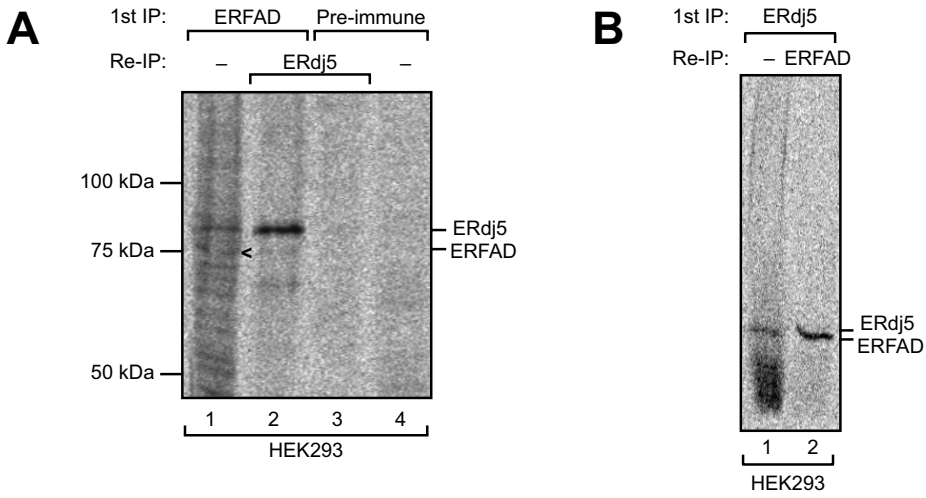

Fig. S3. Complete autoradiographs of the experiments shown in Fig. 2*G*.

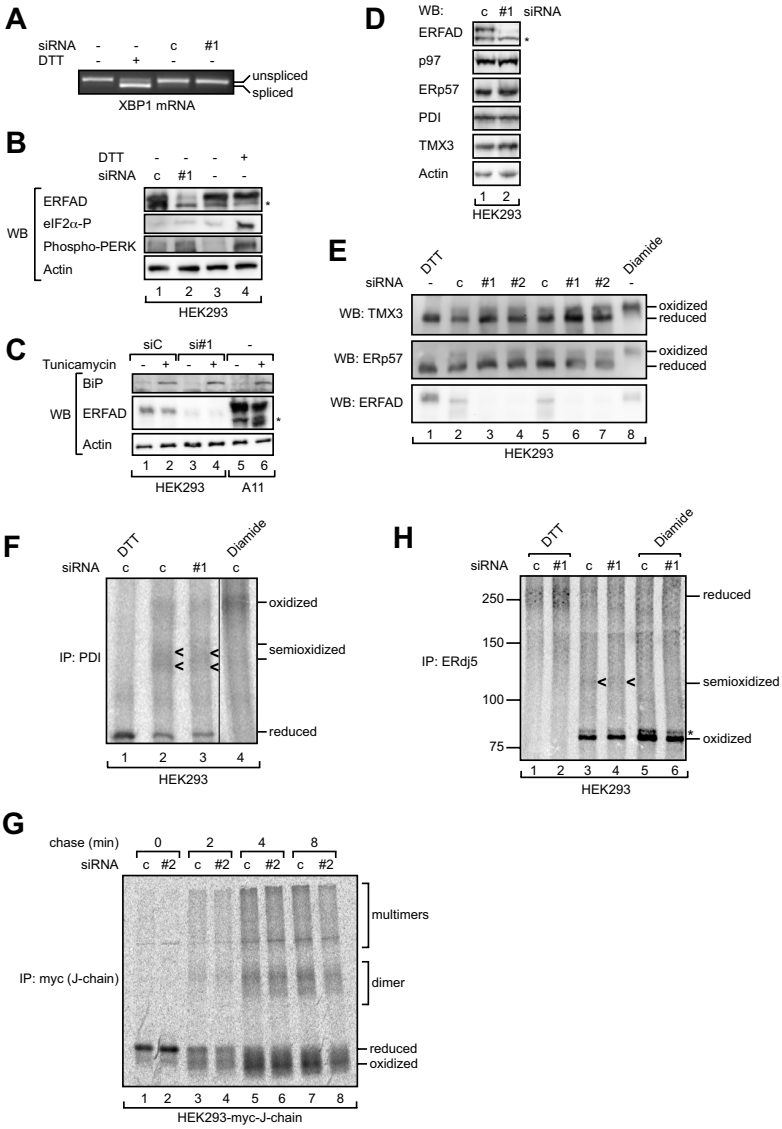

Fig. S4. Knockdown of ERFAD neither significantly induces the UPR nor alters general ER redox homeostasis. (*A*) Effect of ERFAD knockdown on the splicing of XBP1 mRNA. Total RNA was isolated 72 h after transfection with siRNA #1 and control siRNA and reverse transcribed. A PCR with primers specific for XBP1 was performed and analyzed on a 2% agarose gel. An incubation with DTT (2 mM for 1 h) served as positive control. (*B*) Effect of ERFAD knockdown on the phosphorylation state of PERK and eIF2α. HEK293 cells transfected with control siRNA or siRNA#1 were lysed and analyzed in Western blotting with the indicated antibodies 72 h after transfection. DTT incubation (2 mM for 1 h) served as positive control. (*C*) Effect of ERFAD knockdown on BiP induction. As in *B*, except that incubation with tunicamycin (2 μg/mL for 6 h) served as positive control and lysates of A11 cells expressing ERFAD-HA were included in the experiment. (*D*) Effect of ERFAD knockdown on steady state protein levels of p97, ERp57, PDI, TMX3, and actin. Samples were obtained as in *B*. (*E*) Effect of ERFAD knockdown on the redox state of the PDI-family members TMX3 and ERp57. HEK293 cells were transfected with ERFAD siRNA#1 and #2 and nonsilencing control siRNA (c). Seventy-two hours after transfection cells were in situ treated with NEM and lysed. Subsequently, disulfide bonds were reduced and AMS modified. The lysates were analyzed by Western blotting with anti-TMX3, anti-ERp57, and anti-ERFAD. Notice that no significant change in the ratio of oxidized and reduced protein occurred as a results of ERFAD knockdown. (*F*) Effect of ERFAD knockdown on the redox state of PDI. HEK293 cells were transfected with the indicated siRNAs. Seventy-two hours after transfection, overnight pulse labeled cells were lysed after in situ modification with NEM to block free cysteines. Disulfide-bonded cysteines were reduced and then modified with mPEG-mal. Immunoprecipitates of PDI were separated by SDS/PAGE and analyzed by phosphorimaging. Note that the ratio between the different redox forms of PDI did not change between the indicated siRNAs (lanes 2 and 3; arrowheads, semioxidized forms). Incubation of cells with 5 mM diamide and 10 mM DTT for 5 min served as controls for the oxidized and reduced proteins, respectively. The hairline indicates where a lane has been removed from the autoradiograph. (*H*) Effect of ERFAD knockdown on the redox state of ERdj5. As (*F*) except that after overnight pulse labeling cells were directly precipitated in TCA and modified with mPEG-mal before immunoprecipitation with anti-ERdj5 (see also *SI Text*). *, background band. (*G*) The oxidative refolding of immunoglobuling J-chain after DTT washout is not affected by ERFAD knockdown. To probe the oxidative folding capacity of the ER upon ERFAD knockdown, we used the Ig J-chain that has previously been used to assess the effect of Ero1 overexpression (8). HEK293 cells stably expressing myc-J-chain were transfected with ERFAD siRNA#2 and nonsilencing control siRNA (c). Seventy-two hours after transfection the cells were pulse labeled for 5 min in the presence of 5 mM DTT, washed twice at 4 °C, and chased at 37 °C for the indicated times before immunoprecipitation with anti-myc and SDS/PAGE under nonreducing conditions (8). The results showed that after DTT treatment the appearance of the oxidized J-chain monomer occurred with the same kinetics in the absence and presence of ERFAD.

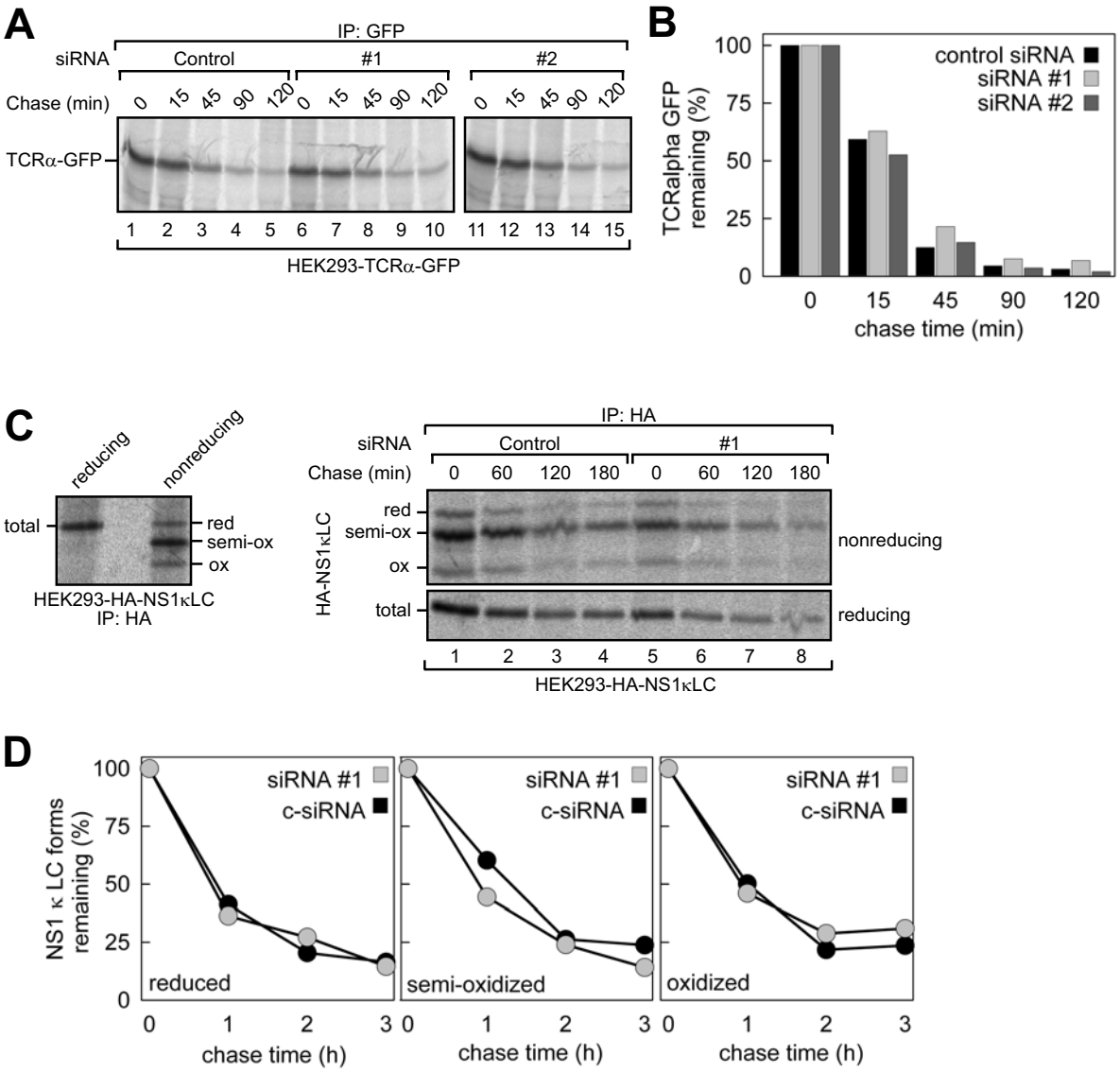

Fig. S5. ERFAD knockdown has no effect on the stability of T cell receptor α subunit (TCRα) and nonsecreted Ig κ LC (NS1κLC). (*A*) TCRα-GFP decay upon ERFAD knockdown. HEK293 cells stably expressing TCRα-GFP were transfected with either siRNA#1 and #2 directed against the ERFAD or nonsilencing control-siRNA (c). Seventy-two hours after transfection cells were pulse-labeled for 20 min and chased for the indicated times. SDS-lysates were subjected to immunoprecipitation with anti-GFP. (*B*) Quantification of the TCRα-GFP decay. The data in *A* were quantified using ImageQuant. The presented experiment is representative for three independent experiments. (*C*) HA-NS1κLC decay upon ERFAD knockdown. HEK293 cells stably expressing HA-NS1κLC were transfected with either siRNA#1 directed against the ERFAD or nonsilencing control-siRNA (c). Seventy-two hours after transfection cells were pulse-labeled for 20 min and chased for the indicated times. SDS lysates were subjected to immunoprecipitation with anti-HA. (*D*) Quantification of the decay of the three redox forms of HA-NS1κLC (reduced, semioxidized and oxidized). The data in *C* were quantified using ImageQuant. The presented experiment is representative for three independent experiments.

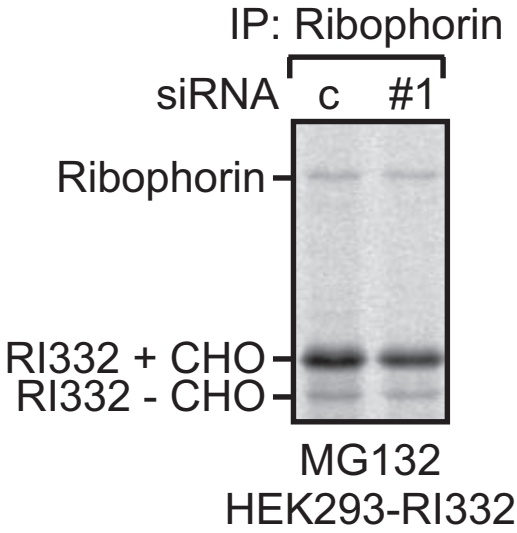

Fig. S6. After pulse labeling, approximately 95% of the newly synthesized RI332 exist in the glycosylated ER form. HEK293 cells stably expressing RI332 were transfected with either siRNA #1 directed against ERFAD or nonsilencing control siRNA (c). Seventy-two hours after transfection cells were pulse-labeled for 10 min in the presence of MG132 without a subsequent chase. SDS lysates were subjected to immunoprecipitation with anti-Ribophorin.

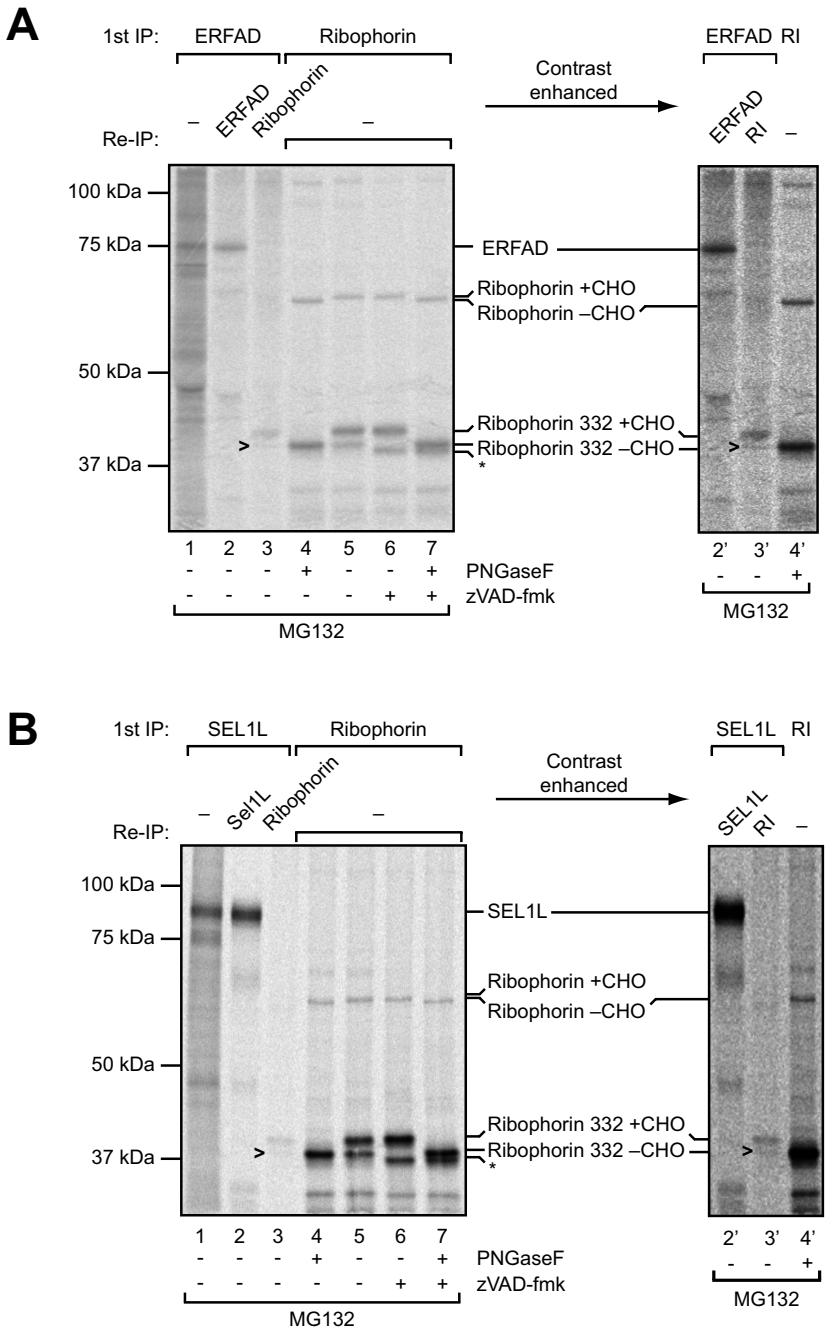

Fig. S7. (*A*) RI_{332} coimmunoprecipitates with ERFAD from lysates of HEK293-RI_{332} cells. As in Fig. 3*E*, except that an additional contrast-enhanced image has been included to better see the precipitated nonglycosylated form of RI_{332}. In addition to the glycosylated form of RI_{332}, a minor amount of a faster migrating form of the protein was observed (arrowhead). To determine the nature of this faster migrating band, we used zVAD-fmk to inhibit Png1 (9). The data showed that RI_{332} appeared as three distinct bands, a glycosylated form (lanes 5 and 6, top RI_{332} band), a deglycosylated form (lanes 4 and 7, middle RI_{332} band), and an as yet unidentified form [lanes 6 and 7, bottom RI_{332} band (∗)]. As judged by gel mobility, the lower band coprecipitating with ERFAD upon MG132 treatment represented deglycosylated RI_{332}. The finding that a minor fraction of deglycosylated RI_{332} precipitated with ERFAD and SEL1L suggests that RI_{332} becomes deglycosylated by the cytosolic Png1 already while in the process of retrotranslocation. Similarly, the ERAD substrate US11 is deglycosylated before complete dislocation while still bound to the ER membrane (10). (*B*) RI_{332} coimmunoprecipitates with SEL1L from lysates of HEK293-RI_{332} cells. HEK293-RI_{332} cells were [^{35}S] pulse-labeled for 5 h in the presence of 5 μM MG132. Anti-SEL1L immunoprecipitates were either analyzed directly (lane 1) or reimmunoprecipitated with anti-SEL1L (lane 2/2′) or anti-ribophorin (lane 3/3′). In lanes 4–7, SDS lysates from cells labeled in the presence or absence of 30 μM of zVAD-fmk (+MG132) were immunoprecipitated with anti-ribophorin with or without subsequent PNGaseF digest to allow the assignment of the three different forms of RI_{332} (RI_{332}+CHO, RI_{332}-CHO and ∗). The arrowhead indicates the minor fraction of deglycosylated RI_{332} (RI_{332}-CHO) interacting with SEL1L.

Table 1. Plasmids and primers

Plasmid	Primer (5′–3′)	Restriction site
pcDNA3/	*forward*: aggcagctgcggccgcaggatgggcctctccgc	NotI
ERFAD-HA	*reverse*: gctctagattagagctcctctttggttcgagcgtagtctgggacgtcgtatgggtagttgctatcgacggactgagc	XbaI
pcDNA5-FRT/	Partial digest of pcDNA3/ERFAD-HA with ApaI (there are two additional ApaI-cleavage sites in ERFAD)	NotI
ERFAD-HA		ApaI
pcDNA3/	*forward*: agcggatccaggatgggcctctccgc	BamHI
ERFAD-His-FLAG	*reverse*: ataagaatgcggccgcttacagttcttccttggttcgcttatcgtcgtcatccttgtaatcatgatgatgatgatgatggttgctatcgacggactgagc	NotI
pRSETminiT/	*forward*: tttggatcctcggtgcccccgcgc	BamHI
His-ERFAD	*reverse*: tctcccatggtcagagctcctctttgttgc	NcoI
pcDNA3/Koza	*forward*: cgaggtaccaacattgtaatgacccaatctcc	KpnI
k-ERp44SS-HA-NSκLC	*reverse*: cgatctagactaacactcattcctgttgaagc	XbaI